ARVO 2023 presentations on Imagine Eyes' retinal imaging

Click on the title to find the abstract in this document. *Times in CET*

rtx1™ Adaptive Optics Retinal Camera

In POSTER session: **Applications of adaptive optics and advanced imaging**

Sun, Apr 23 | 3:45pm - 5:30pm

- A morphometric analysis with adaptive optics imaging of the retinal arterial vascular architecture in RPE65-associated RP patients undergone therapy with voretigene neparvovec
  Friederike Kortuem (Universitat Tubingen, Germany) – abstract 1053 – #C0024
- Evaluating the autofluorescence of the hyper-reflective clumps associated with geographic atrophy in age-related macular degeneration (AMD) with adaptive optics scanning light ophthalmoscopy (AOSLO)
  Natalie Danielsen (University of Pittsburgh School of Medicine, USA) – abstract 1055 - #C0026

In POSTER session: **High resolution and functional imaging**

Sun, Apr 23 | 3:45pm - 5:30pm

- Parafoveal cone loss in inherited retinal dystrophy patients using the rtx1 adaptive optics retinal camera
  Pam Heutinck (Erasmus Medical Center, Denmark) – abstract 1063 – #C0034
- A novel objective method to detect the foveal center point in the rtx1TM device using artificial intelligence
  Amir Akhavanrezayat (Byers Institute, Stanford University, USA) – abstract 1068 – poster #C0039
- Correlation between fixed-luminance flicker full-field electroretinogram response and macular cone density using adaptive optics fundus camera
  Seyed Saeed Mohammadi (Byers Institute, Stanford University, USA) - abstract 1069 – #C0040

In POSTER session: **AMD imaging (advanced AMD)**

Mon, Apr 24 | 3:15pm - 5:00pm

- Deciphering hypereflective foci in age related macular degeneration using adaptive optics in the PINNACLE Study
  Christopher Holmes (Moorfields Eye Hospital NHS, UK) – abstract 2171 - #C0124

In POSTER session: **AMD: Cell Biology, Pathology and Pre-Clinical Studies**

Mon, Apr 24 | 3:15pm - 5:00pm

- Characterizing fixational eye movements in patients with central drusen to find biomarkers for presymptomatic AMD
  Jimmy Murari (Institut de la Vision, France) – abstract 2118 - #C0071

In PAPER session: **AMD: Translational Studies**

Tue, Apr 25 | 3:30pm - 3:45pm

- Exploring the dynamics of pigment in dry AMD through clinical and histological characterization of the RPE
  Yse Borella (Quinze-Vingts National Eye Hospital, France) – abstract 3237

A morphometric analysis with adaptive optics imaging of the retinal arterial vascular architecture in *RPE65*-associated RP patients undergone therapy with voretigene neparvovec

Posterboard#: C0024
Abstract Number: 1053 - C0024

AuthorBlock: *Friederike Charlotte Kortuem[1], Melanie Kempf[1,2], Constanze Kortuem[1], laura kuehlewein[1], Krunoslav Stingl[1], Katarina Stingl[1,2]*
[1]Department of Ophthalmology, Eberhard Karls Universitat Tubingen, Tubingen, Baden-Württemberg, Germany; [2]Department of Ophthalmology, Center for rare diseases, University of Tubingen, Tubingen, Germany;

DisclosureBlock: Friederike Charlotte Kortuem, Code R (Recipient) Novartis, Melanie Kempf, None; Constanze Kortuem, None; laura kuehlewein, None; Krunoslav Stingl, None; Katarina Stingl, Code C (Consultant/Contractor) ProQR, Santen, Janssen, Novartis, ViGeneron

Purpose
To investigate the change of retinal arterial architecture after treatment with voretigene neparvovec in patients with Leber congenital amaurosis type 2 (LCA2) and early-onset severe retinal dystrophy (EOSRD) cause by bi-allelic mutations in the *RPE65* gene.

Methods
All eyes treated at the university clinic of Tubingen, Germany, with voretigene neparovevec received imaging with adaptive optics ophthalmoscopy (AO). However, only six eyes of four patients were able to be follow-up over time due to vast atrophy or malfixation. For each eye five different positions at arterial vessels were selected and the lumen diameter (LD), the wall-to-lumen ratio (WLR) and the wall crosssectional area (WCSA) were measured over an observational period of 12 months with AO.

Results
AO imaging of the retinal vessels in *RPE65*-associated retintis pigmentosa patients is challenging. A vast atrophy dominated all gained AO images. In this study, there were no considerable changes in retinal arterial architecture after treatment with voretigene neparvovec. WLR was constant throughout the observation period. LD and WCSA changed significantly after 2 weeks from the baseline examination. In the follow-up examinations over the period of 12 months LD and WCSA remained stable. There were no signs of inflammation such as macrophages or accumulated fluid visible.

Conclusions
There was no observable inflammatory change of the retinal arterial vasculature over the observation period of 12 months. AO can be used as a diagnostic module to monitor the disease and effects of genetic treatments.

Evaluating the autofluorescence of the hyper-reflective clumps associated with geographic atrophy in age-related macular degeneration (AMD) with adaptive optics scanning light ophthalmoscopy (AOSLO)

Posterboard#: C0026
Abstract Number: 1055 - C0026

AuthorBlock: *Natalie Danielsen[1,2], Valerie C. Snyder[1], Daniel MW Lee[1,2], Ysé Borella[3], Min Zhang[1], Ethan A. Rossi[1,2]*
[1]Ophthalmology, University of Pittsburgh School of Medicine, Pittsburgh, Pennsylvania, United States; [2]Bioengineering, University of Pittsburgh Swanson School of Engineering, Pittsburgh, Pennsylvania, United States; [3]Vision Institute and 15-20 National Ophthalmology Hospital and Sorbonne University, Paris, France;

DisclosureBlock: Natalie Danielsen, None; Valerie C. Snyder, None; Daniel MW Lee, None; Ysé Borella, None; Min Zhang, None; Ethan A. Rossi, Code P (Patent) University of Rochester

Purpose
Hyper-reflective clumps (HRCs) are microscopic structures associated with geographic atrophy (GA) in AMD that were identified with flood-illumination adaptive optics (FIAO). HRCs accumulate within and around GA, migrate at variable rates, and change in number and/or disappear over time. HRCs were hypothesized to be macrophages that accumulated melanin, which is autofluorescent (AF) in the near-infrared (NIR), through the phagocytosis of RPE debris. Here we evaluated the NIRAF of HRCs.

Methods
Five patients with extrafoveal GA were imaged where FIAO had detected HRCs in a previous study (3-4 years ago). All underwent FIAO to determine HRC status and then AOSLO using NIR light (795Δ16) for illumination/excitation. An optical 7-fiber bundle collected confocal and multi-offset light; NIRAF (814–850 nm) was detected in a separate channel. Two patients were imaged 3 months later. Images were registered, averaged, and processed to generate confocal, AF, offset aperture, and multi-offset images; HRCs were segmented manually on FIAO images and compared across modalities.

Results
HRCs were still present in 4/5 eyes and most (85%; n=153/181) were AF. HRCs were hypo-reflective in offset aperture AOSLO but disappeared in multi-offset images. HRC AF signal varied. Most uniformly dark HRCs on FIAO were AF in AOSLO while heterogeneous HRCs showed a smaller area or no AF, occasionally with phase contrast on multi-offset. In the patient with no visible HRCs, several phase contrast objects were seen where HRCs had previously been; nearly all of these had moved by the 3 month follow-up.

Conclusions
Most HRCs were AF and invisible in multi-offset images. The latter suggests they are absorptive as differencing of offset aperture images should cancel the absorptive contrast and enhance the phase contrast. These findings are consistent with the hypothesis that these HRCs contain melanin. However, 15% were not AF, so more work is needed to understand their origin, composition, and evolution. Interestingly, we saw little GA progression and many high contrast phase objects, possibly immune cells, in one patient where HRCs previously had been, suggestive of an adaptive wound-healing response. Further study is needed to understand the interplay between HRCs and macrophages and their relationship to GA progression in AMD.

Parafoveal cone loss in inherited retinal dystrophy patients using the rtx1 adaptive optics retinal camera

Posterboard#: C0034
Abstract Number: 1063 - C0034

AuthorBlock: *Pam Heutinck[1], Danilo Andrade de Jesus[1,2], Luisa Sánchez Brea[1,2], Kubra Liman[1], Daniel Luttikhuizen[1,3], Magda A. Meester[1,3], Marine Durand[4], Theo van Walsum[2], Caroline C W Klaver[5,6], Virginie JM Verhoeven[1,7], Alberta A H J Thiadens[1]*
[1]Ophthalmology, Erasmus MC, Rotterdam, Zuid-Holland, Netherlands; [2]Radiology and Nuclear Medicine, Erasmus MC, Rotterdam, Zuid-Holland, Netherlands; [3]Epidemiology, Erasmus MC, Rotterdam, Zuid-Holland, Netherlands; [4]Imagine Eyes, Orsay, France; [5]Ophthalmology & Epidemiology, Erasmus MC, Rotterdam, Zuid-Holland, Netherlands; [6]Ophthalmology, Radboudumc, Nijmegen, Gelderland, Netherlands; [7]Clinical Genetics, Erasmus MC, Rotterdam, Zuid-Holland, Netherlands;

DisclosureBlock: Pam Heutinck, None; Danilo Andrade de Jesus, None; Luisa Sánchez Brea, None; Kubra Liman, None; Daniel Luttikhuizen, None; Magda A. Meester, None; Marine Durand, Code E (Employment) Imagine Eyes, Theo van Walsum, None; Caroline C W Klaver, None; Virginie JM Verhoeven, None; Alberta A H J Thiadens, None;

Purpose
Retinal imaging using adaptive optics (AO) enables “in vivo” analysis of cone metrics which cannot be attained with other image modalities. In this study, we report our results on parafoveal cone loss in Inherited retinal dystrophy (IRD) patients compared to healthy controls using the rtx1 adaptive optics retinal camera.

Methods
Twenty IRD patients (retinitis pigmentosa n=14, cone dystrophy n=1, Stargardt’s disease (STGD) n=2, Best disease n=1, achromatopsia n=1, central areolar choroidal dystrophy n=1; mean age 51 ± 13 years) and 31 controls (mean age 38 ± 11 years) were enrolled in the study. Our imaging protocol consisted of 2 rows (1.8° and -1.8° degrees vertically) of 7 overlapping images (4°x 4°, 1.5° overlap) from 2° nasal to 14° temporal from the fovea. Cone density and cone spacing were measured using the build-in automated algorithm at 2° and 10.5° temporal eccentricity for both rows. Outer retinal layer (ORL) thickness from OCT was correlated with cone density.

Results
Cone metrics could be obtained in 11 IRD patients and in 18 controls. Measurements were not possible in 9 IRD patients with late-stage disease, due to absent cones and in 13 controls due to low image quality. Between the rows cone metrics did significantly differ at 2° eccentricity for controls (p=0.002). At 2° eccentricity, the mean density and mean spacing were 17253 ± 3293 mm^2 and 8.48 ± 0.89 microns in IRD patients, compared to 21757 ± 1739 mm^2 and 7.51 ± 0.29 microns respectively in controls (p<0.001, p<0.001). At 10.5° eccentricity, the mean density and mean spacing were 11263 ± 4618 mm^2 and 10.85 ± 2.33 microns in IRD patients, compared to 14704 ± 1817 mm^2 and 9.48 ± 1.21 microns respectively in controls (p=0.054, p=0.041). Mean ORL thickness at 2° and 10.5° eccentricity were 86,95 ± 12.59 µm and 78.90 ± 6.67 µm in IRD patients and 84,50 ± 13,40 µm and 80,97 ± 2,94 µm in controls. A significant correlation was found between ORL thickness and cone density (R=0.591, p<0.001).

Conclusions
Cone metrics were significantly reduced in IRD patients at 2° eccentricity compared to controls. Parafoveal cone loss could be accurately measured using our AO imaging protocol in early-stage patients, while this could not be demonstrated with ORL thickness.

A novel objective method to detect the foveal center point in the rtx1™ device using artificial intelligence

Posterboard#: C0039
Abstract Number: 1068 - C0039

AuthorBlock: *Amir Akhavanrezayat[1], Vidya Bommanapally[2], Dilanga Lakshitha Galapita Mudiyanselage[2], Hassan khojasteh[1], Muhammad Sohail Halim[1,3], Chris Or[1], Irmak Karaca[1], Gunay Uludag[1], Negin Yavari[1], Vahid Bazojoo[1], Azadeh Mobasserian[1], YongUn Shin[1], Murat Hasanreisoglu[5,4], Parvathi Chundi[2], Quan Dong Nguyen[1], Mahadevan Subramaniam[2]*

[1]Byers Eye Institute, Stanford University School of Medicine, Palo Alto, California, United States; [2]Computer Science, College of Information Science and Technology, University of Nebraska-Omaha, Omaha, Nebraska, United States; [3]Ocular Imaging Research and Reading Center, OIRRC, Sunnyvale, California, United States; [4]Koç University Research Center for Translational Medicine (KUTTAM), Istanbul, Turkey; [5]Koç University, School of Medicine, Ophthalmology Department, Istanbul, Turkey;

DisclosureBlock: Amir Akhavanrezayat, None; Vidya Bommanapally, None; Dilanga Lakshitha Galapita Mudiyanselage, None; Hassan khojasteh, None; Muhammad Sohail Halim, Code E (Employment) OIRRC, Chris Or, None; Irmak Karaca, None; Gunay Uludag, None; Negin Yavari, None; Vahid Bazojoo, None; Azadeh Mobasserian, None; YongUn Shin, None; Murat Hasanreisoglu, None; Parvathi Chundi, None; Quan Dong Nguyen, Code C (Consultant/Contractor) Belite Bio, Code C (Consultant/Contractor) Genentech, Code C (Consultant/Contractor) Kriya, Code C (Consultant/Contractor) Regeneron, Code C (Consultant/Contractor) Rezolute, Mahadevan Subramaniam, None;

Purpose

rtx1™ is a valuable imaging device for evaluating retinal microstructures. While precise localization is essential, the lack of a gaze tracker and registration system makes device utilization challenging in clinical practice. Currently, a subjective method is employed for the device to detect the central foveal point. Herein, we devised a novel objective method to determine the foveal center point of the eyes using artificial intelligence (AI).

Methods

Seventy-one eyes (38 subjects) were enrolled in our study. Images of five regions of interest (ROI) (4° x 4°) with the central points of (0, 0), (0, -2), (0, +2), (2N, 0), and (2T, 0) were captured and montaged using adaptive optics retinal camera, rtx1™. Spectral-domain optical coherence tomography (SD-OCT) images of all eyes were also captured and considered as a reference to determine the precise location of the foveal center. Two clinicians manually delineated the borders of the fovea based on the blurriness area using both a. tangential (Tg) and b. best-fit sphere (BFS) methods (Figure 1). We also superimposed the montage image of rtx1™ on the images of *en face* OCT manually and marked the OCT-based foveal (OBF) center. We ran the deep learning regression-based model to predict the center points on rtx1™ images based on manually overlayed OCT centers. Ultimately, these predicted AI centers are compared with the OBF, Tg, BFS, and device-based (DB) centers.

Results

The mean age of the participants was 30.9±6.2, and 35% were females. Median distances between OBF points with DB, Tg, BFS, and AI center points were 110.345 (22.28-210.27), 102.44 (69.85-170.3), 106.842 (74-145.82), and 96.2(48.99-134.44) µm, respectively (Figure 2). There was a significant difference between AI and DB center distance from the OB point (p=0.0017). There was no significant difference between the AI center with Tg and BFS center distance from the OBF point (p=0.106,0.06). There were significant differences between the DB with Tg and BFS centers' distance from the OBF point ($p=2.22x10^{-10}$, $3.86x10^{-10}$, respectively).

Conclusions

A novel AI-assisted localization is a helpful method to objectively determine the foveal center quite precisely in AO images which may cover the weakness of the currently used method and may also be beneficial in follow-up-image evaluation.<gwmw style='display:none;'></gwmw>

Layman Abstract (optional): Provide a 50-200 word description of your work that non-scientists can understand. Describe the big picture and the implications of your findings, not the study itself and the associated details.

Accuracy and precision are important factors when we take images of small cells of the back layer of the eye which are called retina cells. Rtx1 is a valuable imaging device that captures the picture of retina cells which enables clinicians to assess and monitor the situation of the back of the eye. Unfortunately, the process of taking images with the rtx1 device is subjective and operator/patient dependent (depending on the patient's compliance and operator skills and experience). Therefore, by using artificial intelligence, we tried to devise a method to make that subjective process into the objective one, in order to increase the level of accuracy and precision of the location of taken images and solve this challenging and crucial issue in a novel and inexpensive way.

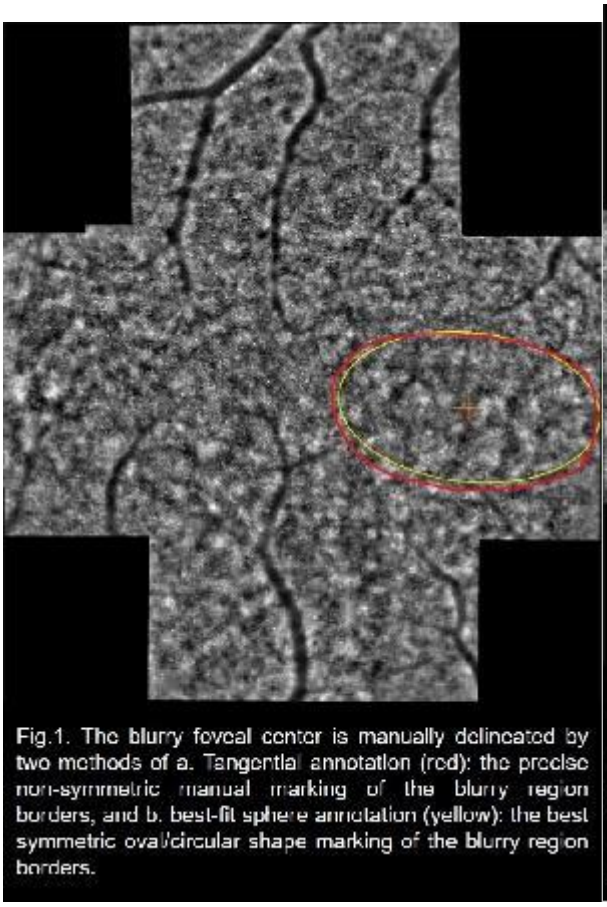

Fig.1. The blurry foveal center is manually delineated by two methods of a. Tangential annotation (red): the precise non-symmetric manual marking of the blurry region borders, and b. best-fit sphere annotation (yellow): the best symmetric oval/circular shape marking of the blurry region borders.

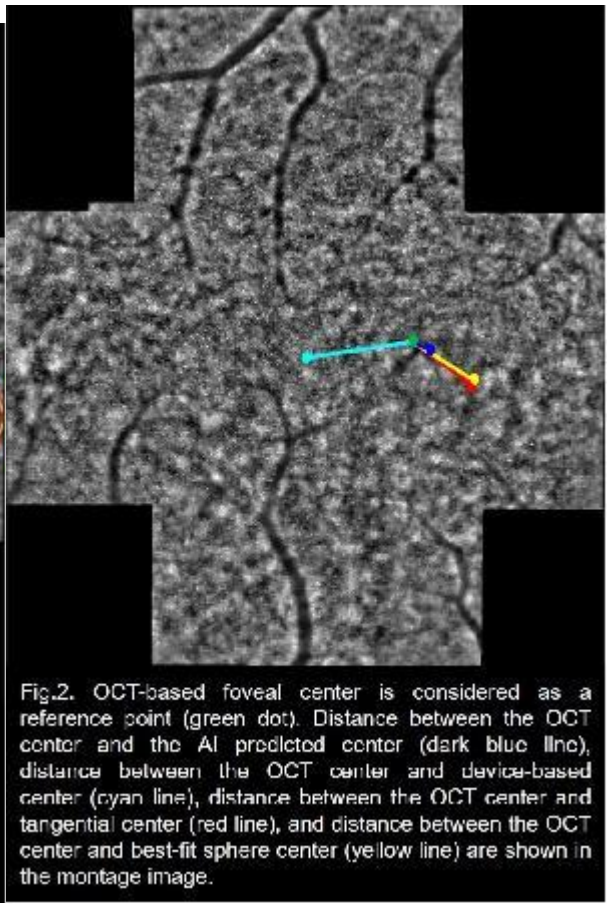

Fig.2. OCT-based foveal center is considered as a reference point (green dot). Distance between the OCT center and the AI predicted center (dark blue line), distance between the OCT center and device-based center (cyan line), distance between the OCT center and tangential center (red line), and distance between the OCT center and best-fit sphere center (yellow line) are shown in the montage image.

Correlation between fixed-luminance flicker full-field electroretinogram response and macular cone density using adaptive optics fundus camera

Posterboard#: C0040
Abstract Number: 1069 - C0040

AuthorBlock: *Seyed Saeed Mohammadi[1], Hassan Khojasteh[1], Negin Yavari[1], Vahid Bajozoo[1], Amir Akhavanrezayar[1], Cigdem Yasar[1], Marine Durand[2], Hashem Ghoraba[1], Irmak Karaca[1], Prapatsorn Ongpalakorn[1], Albert Bromeo[1], Azadeh Mobasserian[1], Xun Lyu[1], Anh Ngoc Tram Tran[1], Diana V. Do[1], Quan Dong Nguyen[1]*
[1]Stanford Medicine, Stanford, California, United States; [2]Imagine Eyes, Orsay, France;

DisclosureBlock: Seyed Saeed Mohammadi, None; Hassan Khojasteh, None; Negin Yavari, None; Vahid Bajozoo, None; Amir Akhavanrezayar, None; Cigdem Yasar, None; Marine Durand, Code E (Employment) Imagine eyes, Hashem Ghoraba, None; Irmak Karaca, None; Prapatsorn Ongpalakorn, None; Albert Bromeo, None; Azadeh Mobasserian, None; Xun Lyu, None; Anh Ngoc Tram Tran, None; Diana V. Do, Code C (Consultant/Contractor) Allergan, Code C (Consultant/Contractor) Genentech, Code C (Consultant/Contractor) Kriya, Code C (Consultant/Contractor) Regeneron, Code C (Consultant/Contractor) Kodiak, Quan Dong Nguyen, Code C (Consultant/Contractor) Belito Bio, Code C (Consultant/Contractor) Genentech, Code C (Consultant/Contractor) Kriya, Code C (Consultant/Contractor) Regeneron, Code C (Consultant/Contractor) Rezolute

Purpose
The correlation between macular cone density (MCD) and flicker electroretinogram (ERG) response is unclear. We hypothesized that a correlation between macular cone density and flicker electroretinogram response might help early diagnosis and detection of retinal disease progression. Therefore, in this prospective case series we aimed to evaluate any possible relationship.

Methods
Twenty-three eyes (12 subjects with no known eye disease) were enrolled in this study. Fixed-luminance flicker full-field electroretinogram (ffERG) responses and MCDs of 24 predetermined loci, excluding the central locus, were measured using Diopsys® NOVA™ and adaptive optics retinal camera (rtx1™, Imagine Eyes, France), respectively (Figure 1A). The MCDs of the center and four adjacent regions of interest (ROI) were measured for each locus using AO Detect Mosaic software (Figure 1B and 1C). Regression analysis was used to evaluate the relationship.

Results
Mean age of subjects was 30 ± 3 years old. Average magnitude of flicker and phase response was 13.44 ± 4.88µV and 332.63 ± 22.12°, respectively. The MCDs of all 24 loci was 15043 ± 3511 cone/mm^2. Maximum and minimum cone densities were both detected on the nasal side, in locations 2N0 (22713 ± 11764 cone/mm^2) and 2N-4 (10858 ± 3945 cone/mm^2), respectively. Among all loci, regression analysis only showed a significant correlation between the cone density of one specific point, locus (0, -4°), and mean magnitude and phase of flicker response (p-values of 0.005 and 0.004, respectively) (Figure 2A and 2B).

Conclusions
In this study, we assessed the potential structural/functional relationship between MCD and ffERG among 24 predetermined macular loci and detected one particular locus in rtx1™ (0, -4°) to be significantly correlated with the ffERG magnitude and phase responses and might be a representative of whole cone cell function. This finding might be beneficial in the early detection of retinal disease progression as well as reduction of the required time to inspect function of entire cone cells.

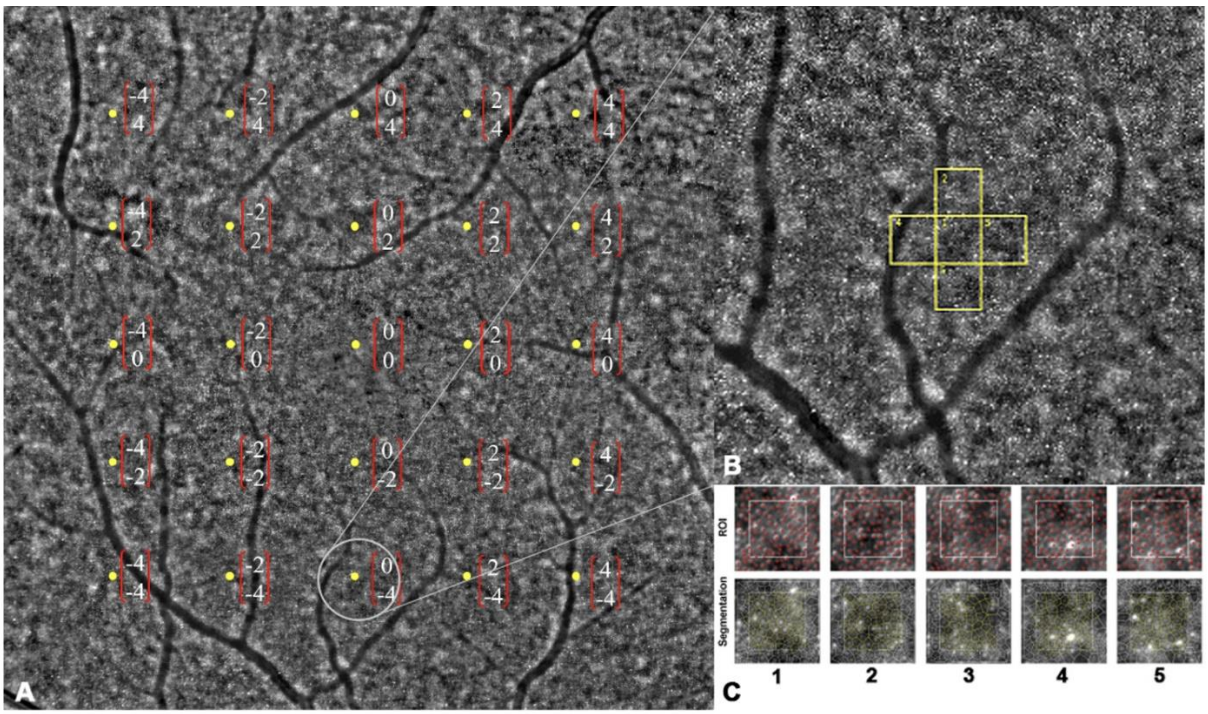

Figure 1. **A** macular cone density was measured in 24 predetermined loci (center locus was unmeasurable). The upper number in the coordinate represents the horizontal location in degree and the lower number represents the vertical one. **B and C** Regions of interest were segmented and analysed by integrated software.

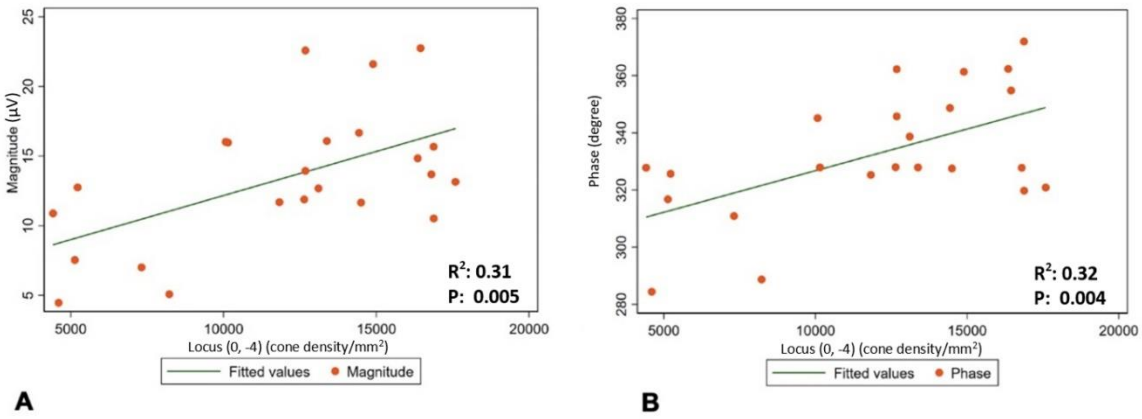

Figure 2. **A** Correlation between cone density in point 0T-4 and mean magnitude of flicker response. **B** correlation between cone density in point 0T-4 and mean phase of flicker response.

Deciphering hypereflective foci in age related macular degeneration using adaptive optics in the PINNACLE Study

Posterboard#: C0124
Abstract Number: 2171 - C0124

AuthorBlock: *Christopher Holmes[1], Syed Ahmer Raza[2], Ahmed M. Hagag[2,1], Thomas Taylor[3], Sophie Riedl[4], Julia Mai[4], Toby Prevost[5], Daniel Rueckert[6], Hrvoje Bogunovic[4], Hendrik P. Scholl[7], Ursula Schmidt-Erfurth[4], Lars G Fritsche[8], Andrew J. Lotery[3], Sobha Sivaprasad[1]*

[1]Moorfields Eye Hospital NHS Foundation Trust, London, London, United Kingdom; [2]Institute of Ophthalmology, University College London, London, London, United Kingdom; [3]University of Southampton, Southampton, Hampshire, United Kingdom; [4]Medizinische Universitat Wien, Wien, Wien, Austria; [5]King's College London, London, London, United Kingdom; [6]Technische Universitat Munchen, Munchen, Bayern, Germany; [7]Institute of Molecular and Clinical Ophthalmology Basel, Basel, Basel-Stadt, Switzerland; [8]Department of Biostatistics, University of Michigan, Ann Arbor, Michigan, United States;

DisclosureBlock: Christopher Holmes, None; Syed Ahmer Raza, None; Ahmed M. Hagag, Code E (Employment) Boehringer Ingelheim, Thomas Taylor, None; Sophie Riedl, None; Julia Mai, None; Toby Prevost, None; Daniel Rueckert, None; Hrvoje Bogunovic, Code F (Financial Support) Heidelberg Engineering, Apellis, RetInSight, Code R (Recipient) Bayer, Apellis, Hendrik P. Scholl, None; Ursula Schmidt-Erfurth, Code F (Financial Support) Genentech, Kodiak, Novartis, Roche, Apellis, RetinSight, Code C (Consultant/Contractor) Apellis, Code P (Patent) RetinSight, Lars G Fritsche, None; Andrew J. Lotery, None; Sobha Sivaprasad, None;

Purpose

Hyper-reflective foci (HRF) on optical coherence tomography (OCT) in age-related macular degeneration (AMD) are seen as hypo-reflective dots (HRDs) in flood illumination Adaptive Optics Ophthalmoscopy (AOO). These HRDs may represent detached retinal pigment epithelial (RPE) and/or inflammatory cells. Microglial activation in AMD may result in outer retinal accumulation of melanosome laden macrophages. Both migrated RPE cells and macrophages may relocate over time, but unlike RPE cells, macrophages can migrate up to 0.02µm/s in healthy retinas and faster (2.37µm/s) when inflamed. We hypothesize that HRDs moving rapidly are more likely to be macrophages than detached RPE, and so we evaluated repeat AOO within hours to determine an HRD's cellular origin.

Methods

Patients with intermediate AMD with HRF in at least one eye were imaged with the rtx1 AO retinal camera at baseline and 1-3 hours later. Overlapping AOO images were taken covering 12° horizontal by 4° vertical, centred on the fovea, and further images centred on areas with high density of HRDs. Images were assessed unedited to minimise image manipulation, and compared to later time points to identify mobile HRDs. Measurements between landmark features with AOdetect software were used to calibrate measurements taken in ImageJ . Macular Spectral Domain OCT scans were obtained in all patients immediately after baseline AOO.

Results

Images from 13 eyes of 12 patients were of adequate quality to assess HRDs. Where individual HRD boundaries were identifiable, mean HRD size was 19.2µm (range: 8.9µm to 36.7µm). Overlapping borders of clustered HRDs made their number, size, and movement challenging to assess in many cases. The majority of HRDs were static within the timeframe of the imaging protocol, but mobile HRDs were found in every image. Assuming linear movement, mobile HRDs travelled at variable speeds, up to 0.036µm/s. Identifying HRFs on OCT corresponding to mobile HRDs was challenging due to clustering and unreliable visibility on OCT, but they were likely outer retinal.

Conclusions

AOO can detect HRD movement in AMD in images captured 1 hour apart. The majority of HRDs were static over periods up to 3 hours, but mobile HRDs were common and faster than previously thought. Mobile HRDs are consistent with activated microglial cells, but the origin of slow HRDs is still unclear.

Characterizing fixational eye movements in patients with central drusen to find biomarkers for presymptomatic AMD.

Posterboard#: C0071
Abstract Number: 2118 - C0071

AuthorBlock: *Jimmy Murari[1], Josselin Gautier[2], Joël Daout[4], Léa Krafft[3], Pierre Senée[5], Pedro Mecê[3], Serge Meimon[3], Michel Paques[2], Angelo Arleo[1]*
[1]Institut de la vision, Paris, Île-de-France, France; [2]Centre Hospitalier National d'Ophtalmologie des Quinze-Vingts, Paris, Île-de-France, France; [3]Office National d'Etudes et de Recherches Aerospatiales, Chatillon, Île-de-France, France; [4]Ecole Polytechnique Federale de Lausanne, Lausanne, VD, Switzerland; [5]Quantel Medical SA, Cournon d'Auvergne, Auvergne, France;

DisclosureBlock: Jimmy Murari, None; Josselin Gautier, None; Joël Daout, None; Léa Krafft, None; Pierre Senée, None; Pedro Mecê, None; Serge Meimon, None; Michel Paques, None; Angelo Arleo, None;

Purpose
We explore Fixational Eye Movements (FEM) at the presymptomatic stages of dry Age-related Macular Degeneration (AMD) by using a new high-speed high-resolution retinal tracking technique. A limited number of studies have linked AMD with quantitative oculomotor markers. We conducted a clinical study to characterize fine spatiotemporal alterations of FEM in patients who start developing foveal drusen but do not have any geographic atrophies.

Methods
Twenty-nine participants were recruited from the SilverSight cohort of the Vision Institute - Quinze-Vingts National Vision Hospital, Paris. They were chosen as part of one of three groups: healthy young adults, healthy older adults, and older adults with foveal drusen.
Drusen were revealed using OCT. Then, gaze-dependent imaging was performed to visualize, count, and measure their diameter and surface on top of thickness. Retinal tracking was based on retinal imaging with an adaptive optics flood illumination ophthalmoscope (AO-FIO). The system allows for sub-arcminute resolution, high-speed, distortion-free images and videos of the retina in the foveal area. It was modified to integrate local stimulation through digital micromirror (DMD) projection deflated from a near infrared source. The DMD was programmed to project stimuli on the retina and perform psychophysics tasks while acquiring a video of the retina at 800Hz. Eye movements were computed using a phase-correlation registration algorithm.

Results
We found statistically significant differences between the drusen group and both healthy young and older adult groups in terms of higher microsaccade amplitude (ANOVA, $p<0.01$), higher drift diffusion coefficient (ANOVA, $p<0.05$), and worse fixation stability -i.e. higher isoline area (ANOVA, $p<0.01$). In the presymptomatic group, drusen eccentricity and density appear to correlate with some FEM attributes such as saccade amplitude and fixation stability.

Conclusions
This study used a novel high-precision retinal tracking technique to better characterize FEM changes as a function of healthy vs. pathological aging. It demonstrated that FEM provide signatures of when the retinal structure begins to get damaged by drusen at the presymptomatic stages of dry-AMD. Overall, central drusen altered fixation stability characteristics, resulting in compensatory FEM changes that could lead to a biomarker for dry-AMD.

Exploring the dynamics of pigment in dry AMD through clinical and histological characterization of the RPE

Abstract Number: 3237

AuthorBlock: *Yse Borella[1,2], Marie darche[1], Anna Verschueren[1], Kate grieve[1], Celine Chaumette[1], Kiyoko Gocho[1], Laila Hmila[1], Jose Sahel[2], Nathaniel Norberg[1], Ethan A. Rossi[2], Michel Paques[1]*
[1]Centre Hospitalier National d'Ophtalmologie des Quinze-Vingts, Paris, Île-de-France, France; [2]UPMC Eye and Ear Institute, Pittsburgh, Pennsylvania, United States;

DisclosureBlock: Yse Borella, None; Marie darche, None; Anna Verschueren, None; Kate grieve, None; Celine Chaumette, None; Kiyoko Gocho, None; Laila Hmila, None; Jose Sahel, None; Nathaniel Norberg, None; Ethan A. Rossi, None; Michel Paques, None;

Purpose
Dry AMD (dAMD) is a frequent and disabling condition affecting the elderly. Mechanisms underlying the progression of atrophy remain largely unknown. Several studies have shown that pigment (melanin) mottling accompanies progression of dAMD. We recently observed that dynamic remodelling of pigment spots in margins moves in synchrony with atrophy progression. Our aim is to understand those dynamics at work in dAMD.

Methods
We analyzed time-lapse sequences from various imaging technologies in 6 patients with dAMD: reflectance and autofluorescence infrared scanning laser ophthalmoscopy, *en face* scleral slab OCT and flood illumination adaptive optics ophthalmoscopy, with or without transscleral illumination. Confocal microscopy of RPE flat-mounts of 7 eyes from 4 donors with dAMD was performed to characterize the mosaic of RPE.

Results
Pigment mottling was present in all patients and showed different aspects by these different modalities. We hypothesize that the appearance of melanin varies by modality due to light- tissue interaction including specular reflectance, scattering, absorption and shadowing (i.e. retroillumination).). In time-lapse sequences, motility of pigment mottling was seen across all modality. Most pigmented spots moved simultaneously to atrophy progression. Interestingly, two different dynamic patterns were visualized: pigment mottling located at the level of the RPE moved with the atrophy bordure whereas the so-called 'hyperreflective foci' located in the neurosensory retina did not show lateral motion. Additionally, intermittent foci of hypertransmission were identified by scleral slab. By confocal microscopy, the mosaic of the diseased RPE was clearly defined and allowed us to map the RPE cell morphology. Transmitted light enabled to document the redistribution of melanin and provided evidence of depigmented RPE cells in every donor eye.

Conclusions
By comparing RPE flat-mounts to *in vivo* en face imaging, a fine characterization of pigment mottling can be obtained. Pigmentary changes may have a variety of origins, and does not necessarily involve RPE cell death. We hypothesize that RPE associated pigment mottling (that we propose to term subretinal HRF) might be a previous state of HRF before it migrates to the inner retina. Those two entities show different dynamic behavior. This approach may help to decipher cellular mechanisms involved in atrophy progression.